



MINISTRY OF TECHNOLOGY

AERONAUTICAL RESEARCH COUNCIL

CURRENT PAPERS

Flight and Tunnel Measurements
of Pressure Fluctuations on the
Upper Surface of the Wing
of a Venom Aircraft with
a Sharpened Leading-Edge

by

R. Rose, *M.Sc. and O. P.* Nicholas, *B.Sc. (Eng.)*

LONDON: HER MAJESTY'S STATIONERY OFFICE

1969

EIGHT SHILLINGS NET

,

,

,

,

,

,

,

,

C.P. 1032 *
November 1967

FLIGHT AND TUNNEL MEASUREMENTS OF PRESSURE FLUCTUATIONS
ON THE UPPER SURFACE OF THE WING OF A VENOM AIRCRAFT
WITH A SHARPENED LEADING-EDGE

by

R. Rose, M.Sc.

O. P. Nicholas, B.Sc.(Eng.)

SUMMARY

Part span sharpened leading-edges were attached to the wing to produce regions of separated flow. Flight measurements were made of both the spectra and root-mean-square intensity of the pressure fluctuations at orifices at 1% and 60% of the local chord. Corresponding measurements on a model in a low speed wind tunnel covered a wider range of incidence and frequency than the flight tests. The flight test results are in good agreement with the tunnel results. The root-mean-square value of the pressure fluctuations, \bar{p} , reached a maximum value of $\bar{p}/q = 0.072$ for the 60% orifice at an incidence of 10° . The incidence for buffet onset was close to that at which the break in the \bar{p}/q vs. α curves for both orifices occurred.

* Replaces R.A.E. Technical Report 67282 - A.R.C. 30135.

CONTENTS

	<u>Page</u>
1 INTRODUCTION	3
2 DESCRIPTION OF AIRCRAFT AND INSTRUMENTATION	3
2.1 The aircraft	3
2.2 Instrumentation	4
3 CALIBRATION ³	6
4 FLIGHT TESTS	6
5 ANALYSIS OF THE MAGNETIC TAPE RECORDS	7
6 RESULTS AND DISCUSSION	8
6.1 Flow visualisation	8
6.2 Icing effects	9
6.3 Power spectra of pressure fluctuations	10
6.4 Root-mean-square pressure fluctuations	11
6.5 Buffet	13
7 CONCLUSIONS	13
Table Venom N.F. 3 - principal dimensions	15
References	16
Illustrations	Figures 1-18
Detachable abstract cards	-

1 INTRODUCTION

Aerofoils have become progressively thinner as aircraft speeds have increased. This has led to an increase in the curvature of the nose section of the aerofoils, and indeed some research aircraft have been designed with sharpened leading-edges. The adverse pressure gradient associated with such leading-edges will cause the upper surface flow to separate; the flow re-attaches at some downstream point on the aerofoil¹. A separation 'bubble' is thus formed and flow unsteadiness associated with this, produces quite large pressure fluctuations on the aerofoil surface. These pressure fluctuations may have significant effects on the buffet characteristics of aircraft and the fatigue of wing panels.

Technique had been developed to measure the total intensity and spectral function of the pressure fluctuations on wind tunnel models² and in flight. Since there was only very meagre information on the character of pressure fluctuations in full-scale flight, a simple flight experiment using a Venom aircraft with part-span sharpened leading-edges was made. The flight tests were made in two phases, the first when only the root-mean-square of the fluctuating pressures was measured: the second when a time history of the pressure fluctuations was recorded on a tape recorder. For comparative purposes, measurements were also made on 2/7 scale model of the Venom at a speed of 150 feet per second in a wind tunnel at R.A.E. Farnborough. The results of these tests were unpublished, but were made in association with overall force and moment tests³.

The work was initiated by Aero Flight Division, and all the flight tests were made at the Royal Aircraft Establishment, Bedford. However, a large part of the experimental work and initial analysis was done by S.C. Roberts whilst at the College of Aeronautics and was used as material for his thesis.

The experimental work was completed in 1960, but, in view of the current interest in separated flow phenomena, publication is warranted.

2 DESCRIPTION OF AIRCRAFT AND INSTRUMENTATION

2.1 The aircraft

The aircraft used for the tests is shown in Fig.1. It is a two-seater Venom Mk.3, powered by a Ghost Mk.104 engine, developing 4850 lb of thrust at sea level. The principal dimensions of the aircraft are given in Table 1.

The **leading-edge** of the wing, between **the** engine intake and the boundary **layer fence** was **sharpened** by the addition of wooden **fairings** attached with **Araldite**, as shown in Figs.2 and 3. To preserve **symmetry**, both wings were modified. In the first place only a small **12-inch spanwise** section between AA and BB of each **wing** was modified; as flight experience was gained and it was found that the modification did not have too large an adverse effect on the aircraft handling characteristics, the sharpened leading-edge was gradually extended to the limits of the intake **and** the fence. **The** aircraft was limited to an equivalent airspeed of 250 knots to avoid over-stressing the Pairing **attachment**. Fig.2 also shows a section of the modified wing at two **spanwise** stations, **AA** and **BB**; **Fig.3a** shows the **fairing** attached to the leading edge of the port wing. The type of profile was chosen to ensure that a separation occurred at low incidence. Pressure orifices, of **3/16** inch diameter, were installed midway between stations AA and BB, at approximately 1% and **60%** of the chord on the upper surface of the starboard wing. For flow **visualisation**, tufts were attached to the upper **surface** of the starboard wing, **Fig.3b**.

2.2 Instrumentation

The pressures at the two orifices on the starboard wing were measured by temperature compensated unbonded strain gauge miniature **Statham** pressure transducers of range $\pm 2.5 \text{ lb/in}^2$ and natural frequency **5.5 kc/s**. These transducers measure differential pressures and **since** only the fluctuating component of the pressure **is** of interest, one side of the transducer was connected directly to the orifice by a short length of $\frac{1}{4}$ inch diameter tube, and the other side to a settling chamber, and thence by 1 mm capillary tubing to the orifice. **This** arrangement **is** shown in Fig.4 and the high lag of the capillary tube ensures that only the **fluctuating** component of the pressure is sensed by the transducers. The natural frequency of the transducers is well above that of the range of the **fluctuating** pressures being measured, and their acceleration **sensitivity is** low.

The output from the transducers was passed through a **zero-adjust** circuit to remove any drift which occurred. This drift, whilst not large in terms of the full scale range of the transducers, was significant, as the **fluctuating** pressures being measured were typically only about **10%** of the range of the transducer. The output was then amplified. The frequency response of the **amplifier** is shown in Fig.5, and is flat up to **80 c/s**, then falls rapidly, due to a low pass filter.

The amplified outputs of the transducer³ could either be recorded as time histories using a frequency modulated signal on a **magnetic** tape recorder or a³ a root-mean-square (rms) value of the fluctuating pressure. The different recordings were made in two series of tests.

The magnetic tape recorder used was **an** eight channel, $\frac{1}{2}$ inch tape recorder, manufactured by the Data Recorder Company. The tape capacity is 900 feet, which, at a tape speed of $7\frac{1}{2}$ inches per second gives a recording time of 24 minutes. The **wow and flutter** of the tape is less than 0.15% rms under laboratory **conditions**. A constant amplitude and **frequency signal** was **also** recorded, to check the **behaviour** of the magnetic **tape** recorder during the high normal **accelerations** and **vibrations** encountered in the flight tests. A fourth track was used to record the pilot's and observer's speech.

The **rms** value of the **fluctuating** pressure **was** measured by a **vacuo-junction***, which consists of a resistance **contained within** a vacuum chamber and a thermocouple to measure the temperature of the **resistance**. The output of the pressure transducer³ was applied, after **amplification**, to the resistance, and consequently **its** temperature **was** proportional to the mean-square of the **fluctuating** pressure. The **vacuo-junctions** were shielded from extraneous temperature effect³ by insulating material. The output³ of the **vacuo-junctions** were recorded by a **Hussenot A.22** recorder.

Normal acceleration, elevator angle, and **incidence** measured by **a vane** mounted on a **nose** boom of the **pitot-static** system, were recorded on another A.22 recorder.

In addition, the following quantities were recorded on an automatic **observer.-**

Indicated airspeed.

Altitude.

Elevator tab angle.

Jet pipe **total** pressure.

Time.

• Footnote a³ a suitable tape recorder was not immediately available the vacua-junction tests were made **first**. At the time the test³ were planned **the technique was relatively untried** in flight. Some of the limitation³ (see section 6.4) of using a **vacuo-junction** to measure the rms of a signal containing **spurious noise** were not fully **appreciated** then.

3 CALIBRATIONS

Steady state calibrations using the two alternative recording systems were made.

The dynamic response of the transducers and associated pneumatic systems was obtained by placing them **behind** a baffle plate in the wall of a wind tunnel, which was run at different wind speeds, and comparing their output with **previously** calibrated transducers. The response of the systems is approximately flat up to 100 **c/s** and 300 **o/s** for the **10%** and **60%** orifices respectively. Above these **frequencies**, the response increases rapidly to a resonant peak at the first fundamental frequency of the **piping**. The effect of these resonances was attenuated by the low pass filter in the amplifier. This effectively limits the useful spectral analysis of the time history records to 100 **c/s**, although the **rms** measurements may **contain** spurious effects due to the resonances in the pneumatic systems at higher frequencies.

The dynamic response of the **vacuo-junctions** is **sluggish**, having a time constant of about 10 seconds.

4 FLIGHT TESTS

Using the magnetic tape recorder, time histories of fluctuating pressure were obtained at two nominally constant speeds at several values of normal **acceleration** penetrating well beyond the buffet boundary. The **recording** time was 90 seconds, giving a **length** of magnetic tape of about **60 feet**, which was the minimum length of tape that could be used on the ground analysis **equipment** to **analyse** accurately the results down to a frequency of 2 **c/s** (see section 5). Records were also taken with the orifices sealed off, to check the vibration **sensitivity** of the whole system. During these tests the tufts on the starboard wing were photographed by the observer, using a hand-held camera.

The **rms** values of the fluctuating pressures were measured over a somewhat **wider** range of **conditions**, at both **10000 feet** and **30000** feet. Fig.6 shows the flight envelope covered; the Reynolds numbers quoted are **mean values** $\pm 1 \times 10^6$. It was necessary to hold conditions steady for about 30 seconds prior to the **recordings**, to allow the observer to adjust the zero circuits and give the vacuo-junctions time to stabilise. The **recordings** were not so accurate at the higher values of normal acceleration and more severe buffet intensity, as the zero adjusting was difficult under these conditions. To

extend the range of Reynolds number and Mach number, **some** tests were made in level flight at various altitudes up to 37000 feet. The aircraft buffet levels were also determined, based on pilots' assessments.

5 ANALYSIS OF MAGNETIC TAPE RECORDS

The method of analysis of the tape records and the equipment used is essentially similar to that used by Owen² and thus only an outline is given here.

The root-mean-square value of the pressure fluctuations over the spectrum is \bar{p} , and this is made non-dimensional by dividing it by the dynamic pressure, q ($=\frac{1}{2}\rho v^2$).

A non-dimensional frequency parameter is defined as

$$n = \frac{f \ell}{v},$$

where f = frequency in cycles per second,

ℓ = a representative length, taken as the local chord of the wing at the measuring station,

v = free stream velocity.

A spectral function $F(n)$ is defined, such that $F(n) dn$ is the contribution to $(\bar{p}/q)^2$ in the frequency range n to $n + dn$.

Thus

$$d \left(\frac{\bar{p}}{q} \right)^2 = F(n) dn = n F(n) d(\log n).$$

The results of the spectral analyses can therefore be plotted in the form of $F(n)$ against n , or $n F(n)$ against $\log n$; and, in either case, integration over any range of frequency gives the corresponding mean-square intensity of the fluctuation. In particular, the total area under either curve is equal to the total intensity for

$$\left(\frac{\bar{p}}{q} \right)^2 = \int_0^{\infty} F(n) dn = \int_0^{\infty} n F(n) d(\log n).$$

The spectra measured generally covered a wide range of frequency and thus it is more convenient to present results in the form of $n F(n)$ vs. $\log n$.

The spectra were **analysed** to give the spectral function $F(n)$ using a **Muirhead-Pametrada D-489 analyser** which covers the frequency range 20 to 20000 c/s. The low frequency range was extended to include the range 2 to 20 c/s by introducing a low frequency modulator. In fact, the **records** should not contain any significant content above 100 c/s because of the low-pass filter in the amplifier used to augment the signals from the pressure **transducers**. The magnetic tape records were formed into loops for the analysis. Experience in the analysis of wind tunnel **results**² has shown that at least 150 cycles of the lowest frequency to be **analysed** must be contained within the loop; **in the** present test the minimum length of the loops is 60 feet, **which** contains about 180 cycles of the lowest frequency that could be **analysed**.

6 RESULTS AND DISCUSSION

6.1 Flow visualisation

Fig.7 shows a **photograph** obtained **from** the hand held camera of the surface **tufts** on the starboard wind under typical test conditions. Outboard of the boundary **layer** fence the flow is, **as** expected, attached. However, inboard of the fence behind the sharpened leading-edge, the flow has separated over a considerable portion of the chord; large regions of reverse **flow** are shown by the tufts pointing upstream.

This type of bubble separation **for aerofoils** with sharp leading edges had been observed in wind **tunnels**² and has since been studied **extensively**⁴. The flow re-attaches behind the bubble; the point of re-attachment depends on the Incidence and Reynolds number since these effect the point in the **larinar** shear layer where transition occurs. Unsteadiness of the bubble **can** occur giving rise to fluctuating pressures on the **wing** surface.

The behaviour of the surface tufts has been used to define the position of the re-attachment line. Because of the simplicity of the method the line cannot be defined to better **than** 5% local chord and at the highest lift coefficients tested much less accurately, due to the large fluctuations in the bubble length. Fig.8 shows a typical contour of the separation bubble which starts near the **intake** lip **and** terminates at the boundary layer fence. The flow in the outboard part of the bubble is approximately two-dimensional, but near the intake three-dimensional effects **are** present.

Fig.9 shows the variation of bubble length, at the **spanwise** transducer station, with **aircraft lift coefficient** for various flight conditions. The bubble varies in length from 20% chord at the lowest lift coefficient tested, $C_L = 0.2$, to a **full** chord separation at lift coefficients of the order 0.6. There may be a systematic variation, for a given C_L , of the bubble length with Reynolds number, but **in** view of the difficulty of defining the xx-attachment point at high lift coefficients and the relatively small range of Reynolds number covered **in** the tests no definite conclusions can be drawn. Also it should be noted that the lift coefficient is the mean for the wing, which is not necessarily the **same** as the local value for the sharpened leading-edge section. Fig.9 also shows results deduced from original **tuft** film records **taken** during tunnel **tests**³ and these are in reasonable agreement with the flight results showing that scale effects are small, although the separation bubble reaches the trailing-edge at a slightly lower incidence in flight,

6.2 Icing effects

On one of the flights the aircraft was climbing slowly through **4000 feet** at an **indicated** airspeed of **140** knots. The tufts on the starboard wing were pointing forwards showing that the flow on the **modified** wing section was fully separated, the buffet level was severe, and a stick force to trim of approximately 30 lb pull was required. Suddenly a very large trim change **occurred** requiring a push force of 30 lb to trim, the buffet intensity was reduced considerably, and the tufts indicated a flow re-attachment at about **70%** chord. When the power was reduced **and** the aircraft allowed to descend slowly through **4000** feet the reverse occurred. This process was repeated several times and the **behaviour** was found to be most consistent.

On the day of this test the icing level was at **4000 feet** and the weather was good **with** little cloud. Although no icing was observed a possible explanation of the occurrence is the formation of a small amount of ice on the leading edge, **which** would increase its radius and thus reduce the size of the bubble. Another explanation could be that ice crystals in the **air** promoted an earlier transition than usual in the **laminar** shear layer, thus **reducing** the bubble size. This seems less likely **since** the data in this Report show that quite large changes in Reynolds number have little effect on the flow.

6.3 Power spectra of pressure fluctuations

For the flight results the low pass filter begins to cut off at 80 c/s and thus the flight spectra have not been analysed beyond about 100 c/s. Hence the more extensive wind tunnel spectra are discussed first followed by a comparison with flight results.

Fig.10 shows the spectra of the pressure fluctuations at the 10% orifice measured in the wind tunnel for incidences from 0° to 14° . As incidence is increased from zero the spectra show a primary peak in $n F(n)$ at gradually reducing values of n . The maximum value of this primary peak is 0.0017 and occurs at an incidence of 3° when the separation bubble length (Fig.9) is about 15% of the local chord. As the Incidence is Increased further up to 7° the maximum value of the primary peak decreases and the energy of the spectra is reduced. At 8° incidence a secondary peak develops at about $n = 0.35$ and the primary peak disappears. At 10° , when Fig.9 shows that the separation bubble is approaching the trailing edge, the secondary peak at about $n = 0.1$ increases rapidly and the spectral energy increases rapidly. With further increase of incidence the flow no longer re-attaches to the wing surface, and this causes a reduction in the secondary peak until at an incidence of 14° the spectrum is quite flat.

Fig.11 shows spectra for the 60% orifice for the tunnel tests from $a = 0^\circ$ to 14° . As incidence is increased from zero a primary peak develops with the same characteristics as noted for the 10% orifice although the peak values are much larger. The primary peak reaches a maximum value of about 0.0125 for an incidence of 11° at about $n = 0.5$; this primary peak persists until at least 12° . A secondary peak first appears at 8° at about $n = 0.15$, this secondary peak reaches a maximum at an incidence of 10° . At 14° both the primary and secondary peaks persist, but are much smaller.

Comparisons of the spectra measured at the 10% and 60% orifices show certain similarities. As incidence is increased a primary peak develops at gradually reducing values of n . The maximum value of this peak is approximately proportional to the orifice distance from the leading edge and occurs when the orifice position is about two-thirds of the separation bubble length. As the separation bubble approaches the trailing edge a secondary peak develops rapidly, this has the same value for either orifice and occurs at a reduced frequency of just greater than 0.1. As the incidence is increased

further and the flow no longer re-attaches to the wing ~~the~~ energy in the spectra ~~is~~ reduced rapidly.

The power spectra of the pressure fluctuations measured in flight for the ~~10%~~ and ~~60%~~ orifices are shown in Figs.12 and 13 at various lift coefficients. ~~As~~ explained previously the spectra have not been ~~analysed~~ at high frequencies and thus only a limited comparison with the tunnel data ~~is~~ possible. For the ~~10%~~ orifice the primary peak is cut off, but the secondary peak develops in a ~~manner similar~~ to ~~that~~ indicated by the tunnel results. In the case of the ~~60%~~ orifice the spectra measured in flight cover both primary and secondary peaks ~~and~~ the results are similar to those of the tunnel tests.

The good agreement between the flight and tunnel results for a sharp ~~leading~~ edge suggests that at least at up to subsonic speeds of the order $M = 0.7$ ~~and~~ Reynolds numbers of about 20×10^6 , satisfactory scaling laws from low speed ~~wind~~ tunnel tests can be established and the effects of Reynolds number, Mach number, tunnel turbulence ~~and~~ aircraft flexibility are small.

6.4 Root-mean-square pressure fluctuations

The spectra of the pressure fluctuations have been integrated to obtain the root-mean-square (rms) level of the pressure fluctuations \bar{p} , and these have been ~~non-dimensionalised~~ in Figs.14 and 15 for the ~~10%~~ and ~~60%~~ orifice respectively.

The flight results have been integrated over the maximum available range of the ~~reduced~~ frequency parameter, n , 0.05 to 1.0. For comparative purposes the tunnel results have been integrated over the same range as the flight results and over the 'full' range 0.05 to about 30; integration to lower reduced frequency values was not possible due to limitations of the analysis equipment at low frequencies. The spectral shapes suggest that terminating the full range integration at an n of about 30 does not exclude any appreciable energy.

The full integration of the tunnel results for the ~~10%~~ orifice, Fig.14, shows that \bar{p}/q increases from zero at 0° incidence to a peak of 0.016 at 3° and another peak of 0.037 at 11° . These two peaks correspond to the ~~primary~~ and ~~secondary~~ peaks noted in the spectra, Fig.10. At 14° incidence \bar{p}/q has fallen to 0.005. The integration of the tunnel results over the truncated

range $n = 0.05$ to 1.0 is broadly similar except that the maximum value of the first peak is lower due to the out-off at $n = 1.0$ eliminating the major content of energy of the primary peak. The flight results are only available for a small range of incidence, but these are in quite good agreement with the comparable tunnel results.

For the 60% orifice the full integration of the tunnel results, Fig.15, shows that \bar{p}/q increases from zero at $\alpha = 0^\circ$ to a single peak value of 0.072 at 11° falling to 0.020 at 14° . The integrated results of the tunnel spectra over the truncated range $n = 0.05$ to 1.0 are very similar because little energy exists above $n = 1.0$. Here the flight results cover most of the tunnel incidence range and are in very good agreement with the tunnel tests.

It should be noted that the maximum values of \bar{p}/q are much larger than the normally accepted value of about $0.006 q^{5,6}$ for attached turbulent boundary-layer flow.

The rms pressure fluctuations were also measured by the vacuo-junctions and the results expressed in terms of \bar{p}/q are shown in Figs.16 and 17 for the 10% and 60% orifices respectively. These results are compared with the integrated spectra in Figs.14 and 15. It is apparent that whilst the vacuo-junction and integrated results show similar trends with incidence, the vacua-junction results are much larger. The results from the vacuo-junctions are almost certainly spurious, and the most likely reason is background noise in the system in flight. The spectral analysis of the tape records was limited to frequencies where the response was flat, i.e. below 100 c/s and noise at any frequency above this would not have been noticed, even if it was on the tape. Resonances at 300 c/s and 600 c/s associated with the 10% and 60% orifices respectively may have contributed to the signals, despite the nominal cut-off of the amplifiers at 100 c/s. The vacuo-junction has a very high frequency response and could also have responded to any noise beyond the upper limit of the tape deck (about 2 kc/s). Thus the vacua-Junction results are regarded as unreliable and show that great care must be taken when measuring the overall level of pressure fluctuations. If such an automatic integrating system is used it is essential to filter the signals first so that they are confined to the frequency range of interest, and to make a spectral analysis to confirm that the filter effectively suppresses any signals including resonances or noise outside this frequency range.

In spite of the limitations of the **vacuo-junction** tests they were of some use. They showed that a significant pressure fluctuation built-up with incidence and thus it was worthwhile proceeding with **the** more complex spectra measurements.

6.5 Buffet

Pilots' assessments of the aircraft's buffet levels are shown in **Fig.18**, together with the boundary for appreciable buffet on the original aircraft. For the modified aircraft buffet onset is at a CL of about 0.35 ($\alpha \approx 5.5^\circ$) and varies little **with** Mach number. Thus below $M = 0.65$ the addition of the part-span sharpened leading-edge roughly halves the CL for **appreciable** buffet, and almost **completely** suppresses the dependence of buffet level upon Mach number.

It is interesting to note that, omitting the initial peak at low **inci-**
dence in the tunnel results for the 10% orifice, the onset of increasing \bar{p}/q derived from any of the sets of data in Figs.14 or 15 is at an incidence **between** 6° and 7° . Thus \bar{p}/q vs. α from any of the sets of tunnel or flight data, including the suspect **vacuo-junctions**, would provide an adequate **indica-**
tion of buffet onset on the modified **aircraft**.

However it should be noted that for the Venom, the wing fundamental bending frequency is about 8 c/s, and the frequency corresponding to the secondary peak in the spectrum is at 4.5 to 9.0 c/s for Mach numbers from 0.3 to 0.6. Thus the **break** in the \bar{p}/q vs. α curves, which corresponds to the growth of the secondary peak, shows the onset of **excitation** at near a structural frequency in the present tests. Caution should be used in applying this result in cases where the aerodynamic and structural frequencies **are** not closely matched.

For a similar range of flight conditions the primary **spectral** peak occurs in the frequency range **between** 20 and 200 c/s and thus could affect panel fatigue.

7 CONCLUSIONS

The part span sharpened leading-edge fitted to the Venom wing produced a separation of the flow on the upper surface. This separation re-attached before the trailing edge at low **incidences**, but the re-attachment point moved aft as incidence increased until eventually at about an incidence of 10° the flow failed to re-attach to the wing.

The spectra of pressure fluctuations at two orifices at 10% and 60% of the local chord within the separated flow agreed well in the flight and low-speed wind tunnel tests. This suggests that at least for a sharp unswept leading edge up to a Mach number of 0.7 and a Reynolds number of 20×10^6 satisfactory scaling laws can be established from low-speed tunnel tests and that the effects of Reynolds number, Mach number, tunnel turbulence and aircraft flexibility are small. The characteristic variation of the spectra with incidence and chord position were established, but they are probably specific to the particular configuration tested. Integration of the spectra gave root-mean-square values of the pressure fluctuations \bar{p}/q that reached maximum values of 0.037 and 0.072 for the 10% and 60% orifices respectively at an incidence of 11° as the separation bubble reached the trailing edge. Results of an attempt to measure root-mean-square pressure fluctuations directly using a vacuo-junction were not reliable, probably due to background noise in the system in flight. The incidence for buffet onset was close to those at which the break in the \bar{p}/q vs. α curves for both orifices in tunnel and flight, including the suspect vacuo-junctions, occurred.

On one flight considerable changes of longitudinal trim and buffet, associated with changes in size of the separation bubble, were experienced as the aircraft climbed or descended through the icing level. These effects may have been caused by small amounts of ice forming on the sharp leading-edge, although none was observed.

TableVENOM N.F. 3 - PRINCIPAL DIMENSIONSWing

Area	279 feet ²
Setting relative to fuselage datum	0 degrees

Dihedral 3 degrees

Leading-edge sweep 17.1 degrees

Span 41 feet

Aerofoil section (unmodified): symmetrical section, **maximum thickness/chord** 0.1, at 0.4 **chord**.

Tailplane (including elevator)

Area	52.3 feet ²
Mean weight during tests	11500 lb

REFERENCES

<u>No.</u>	<u>Author</u>	<u>Title, etc.</u>
1	P.R. Gwen L. Klanfer	On the laminar boundary layer separation from the leading edge of a thin aerofoil. A.R.C. C.P. 220 (1953)
2	T.B. Owen	Techniques of pressure fluctuation measurements employed in the R.A.E. low speed wind tunnels. AGARD Report 172, (A.R.C. 20780) (1958)
3	M.B. Guyett	Low speed wind tunnel tests on the De Havilland Sea Venom with a part-span sharp wing leading-edge extension. R.A.E. Technical Note Aero 2644 (A.R.C. 21823) (1959)
4	V. Gaster	The structure and behaviour of laminar separation bubbles. N.P.L. Aero Report 1181, (A.R.C. 26226) (1966)
5	D.R.3. Webb A.R. Keeler G.R. Allen	Surface pressure and structural strains resulting from fluctuations in the turbulent boundary layer of a Fairey Delta 2 aircraft . A.R.C. C.P. 638 (1962)
6	E.J. Richards M.K. Bull J.L. Willis	Boundary layer noise research in the U.S.A. and Canada - A critical review . U.S.A. A. Report 131, (1966)

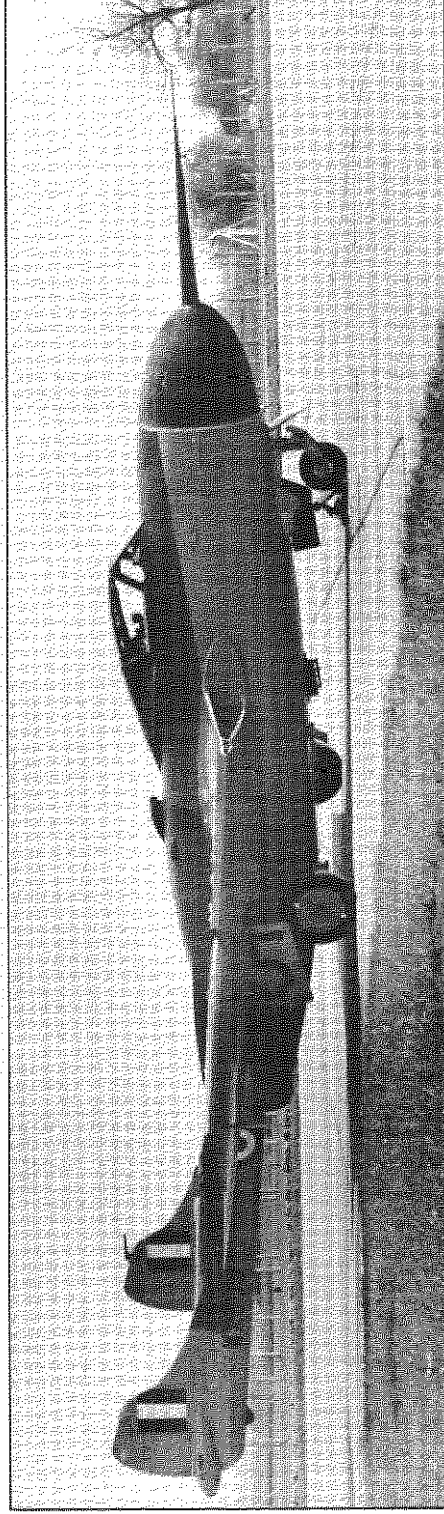
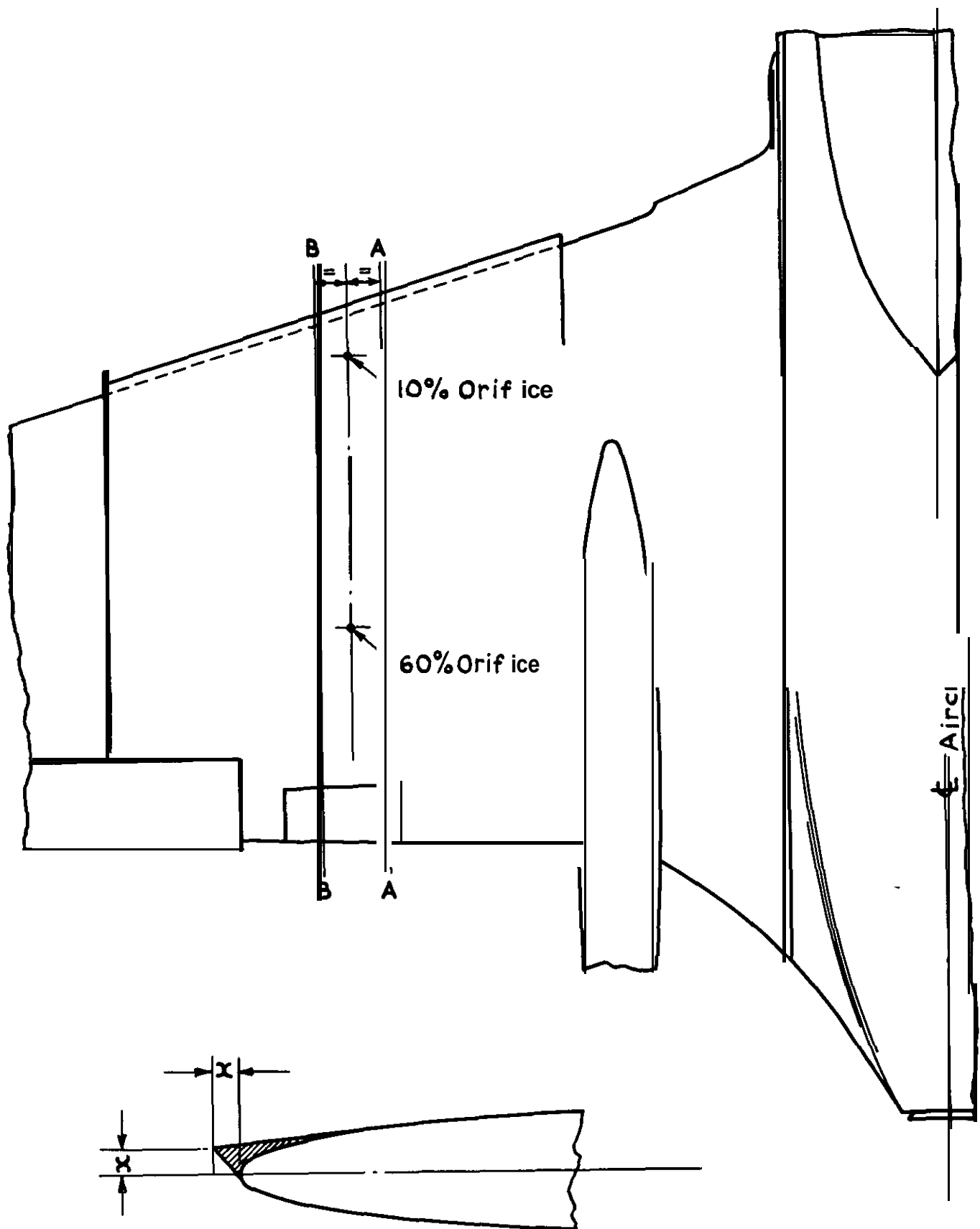


Fig.1 View of Venom aircraft with modified wings



At Section A-A $x = 1.88$ in

At section B-B $x = 1.80$ in

Local chord at measuring station = 96 in

Fig. 2 Details of sharpened leading-edge

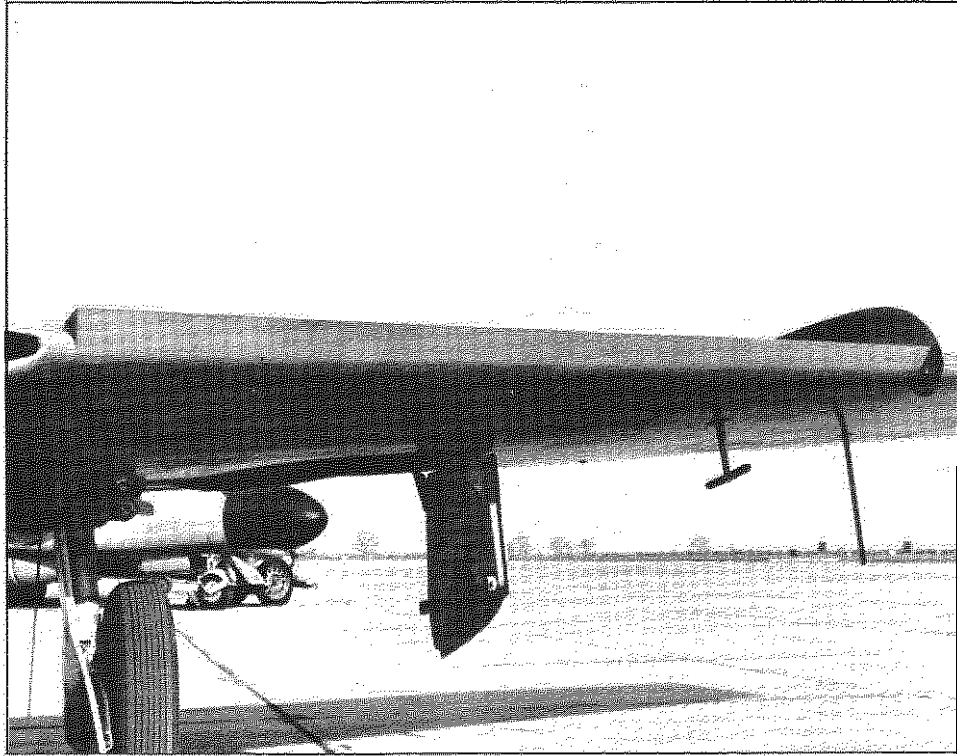


Fig.3(a) Port wing, showing sharpened leading edge

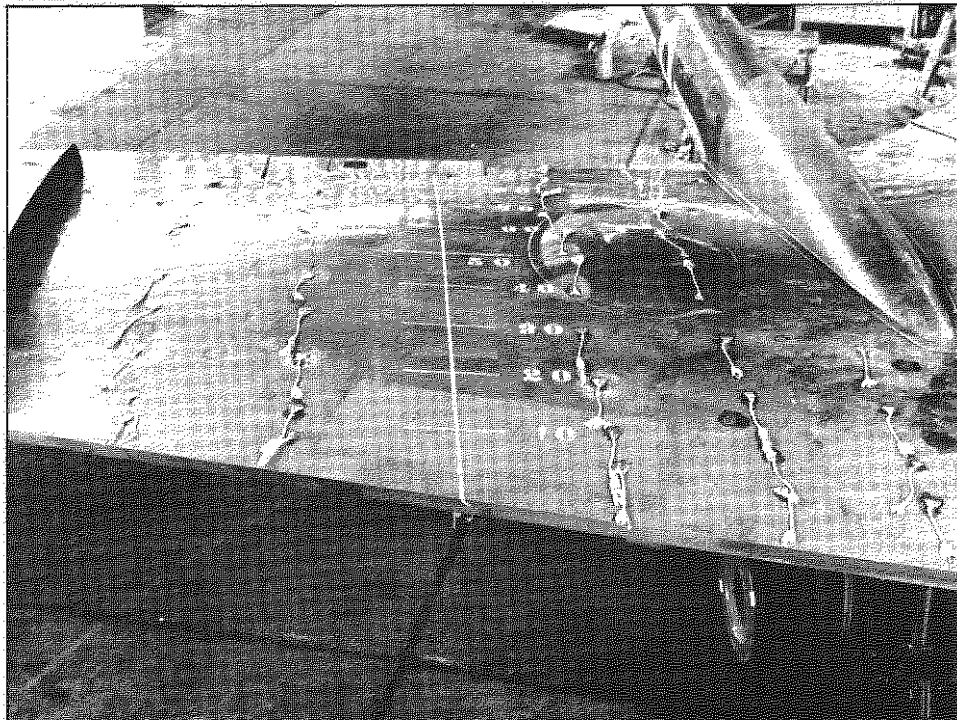


Fig.3(b) Upper surface of the starboard wing, showing tufts

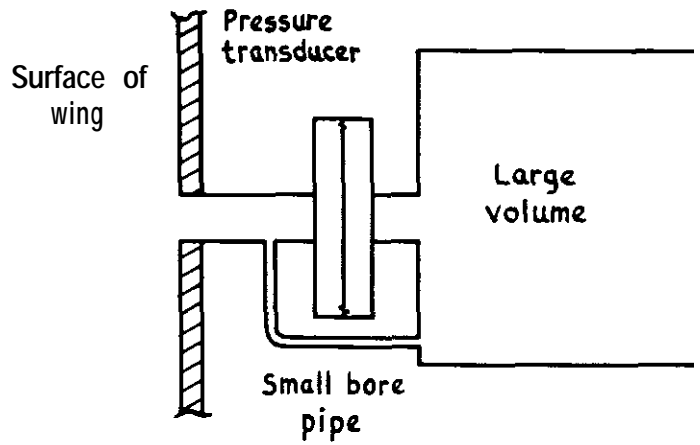


Fig.4 Schematic diagram of transducer installation

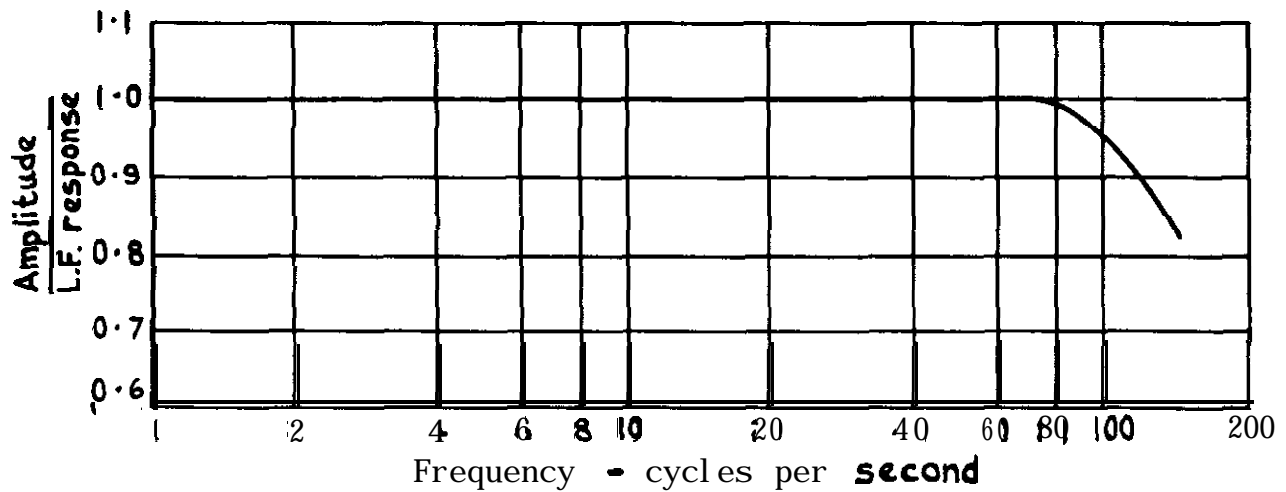


Fig. 5 Amplifier frequency response

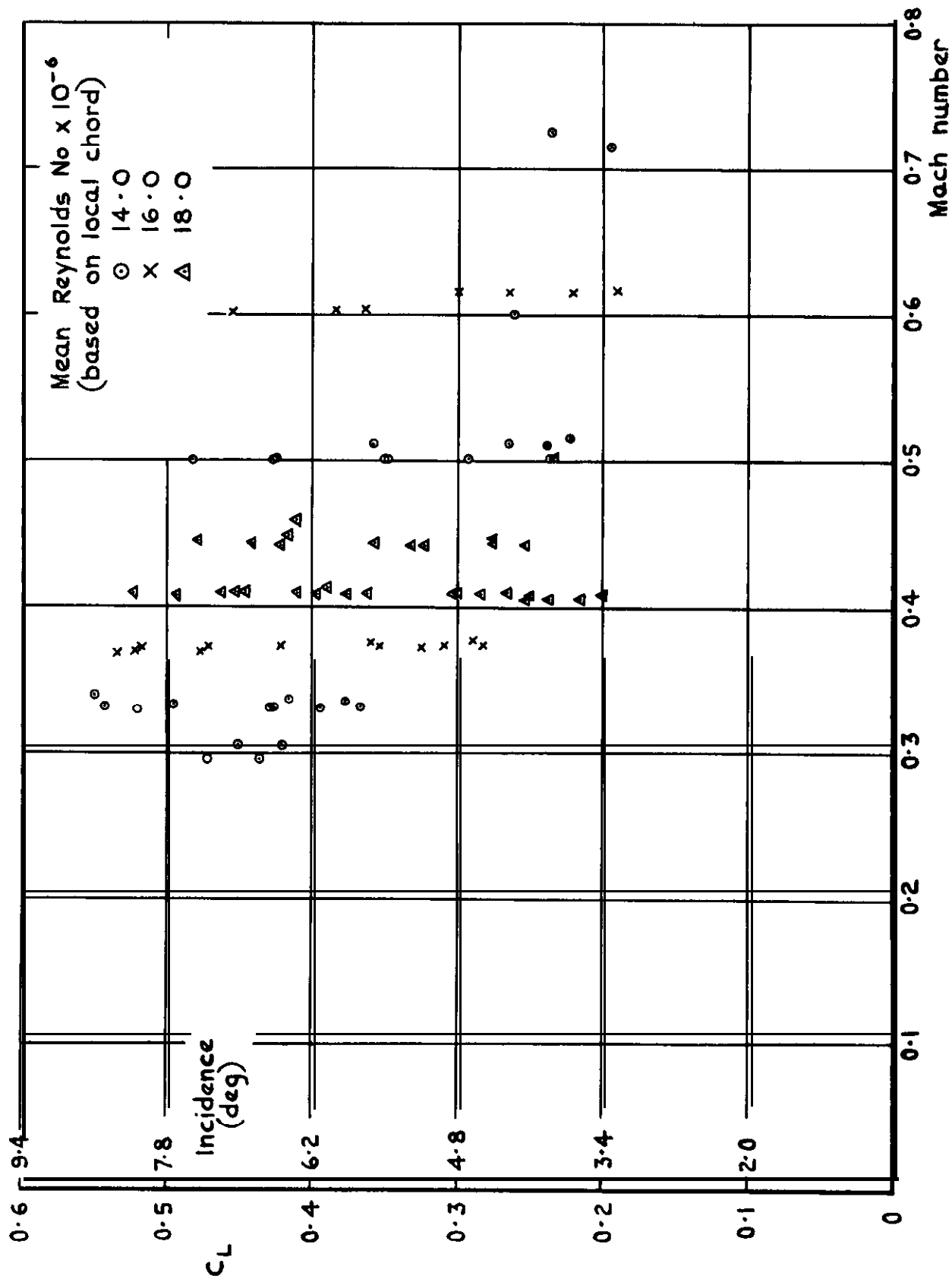
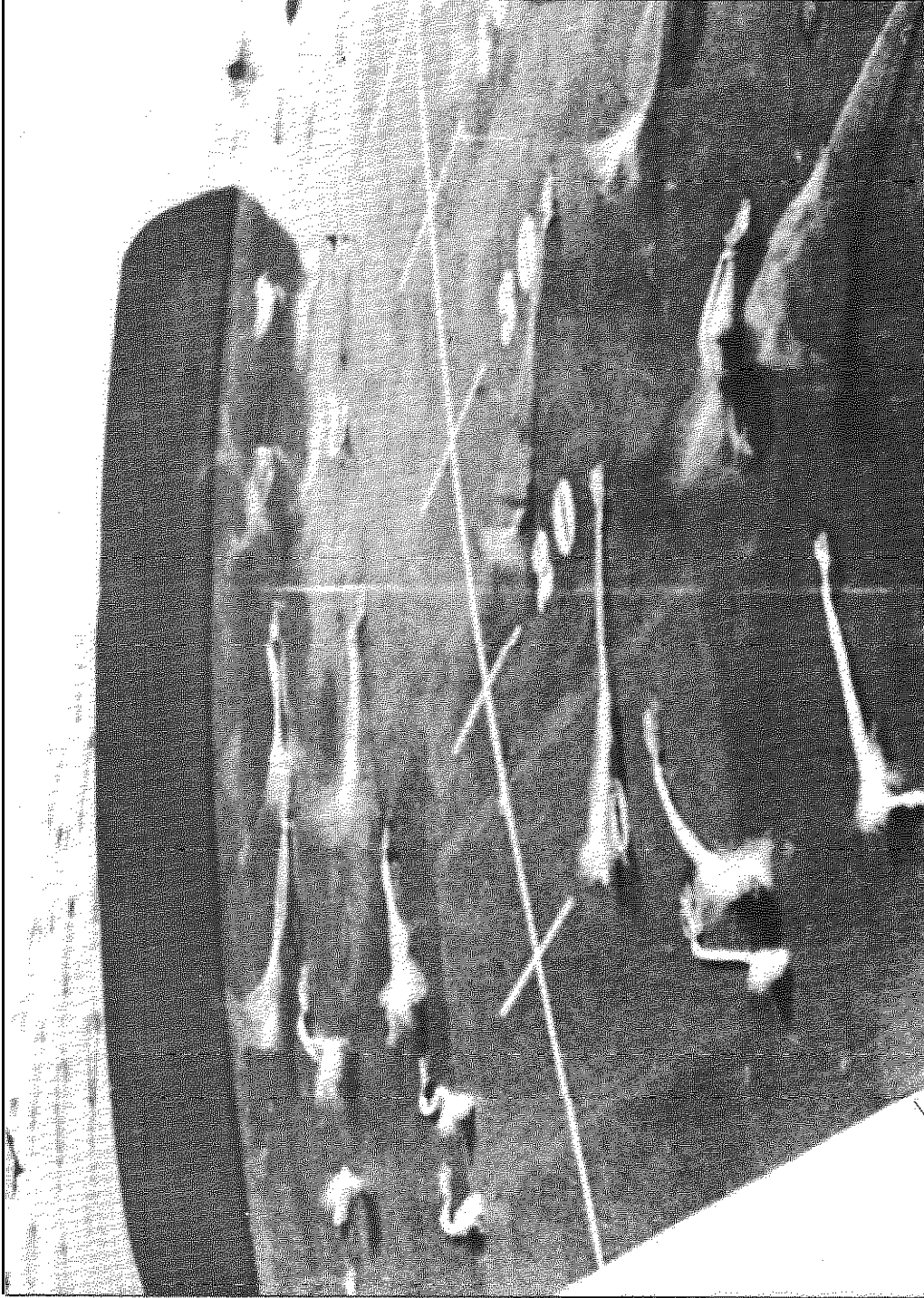


Fig. 6 Flight envelope of RMS pressure measurement tests



Leading edge

Fig.7 Typical flow pattern over the wing at C = 0.35

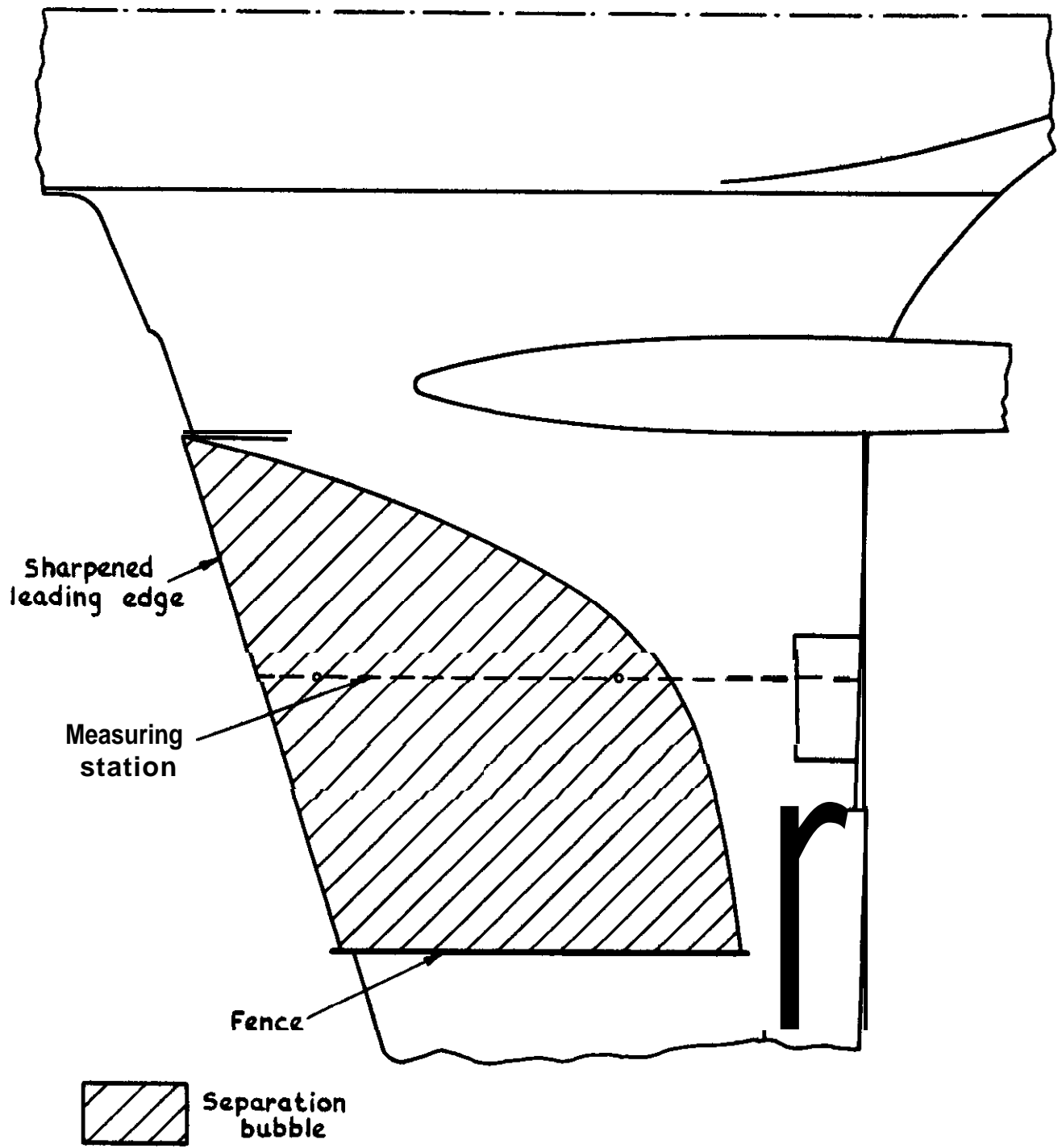


Fig. 8 Typical contour of the separation bubble at $C_L \approx 0.5$ in flight

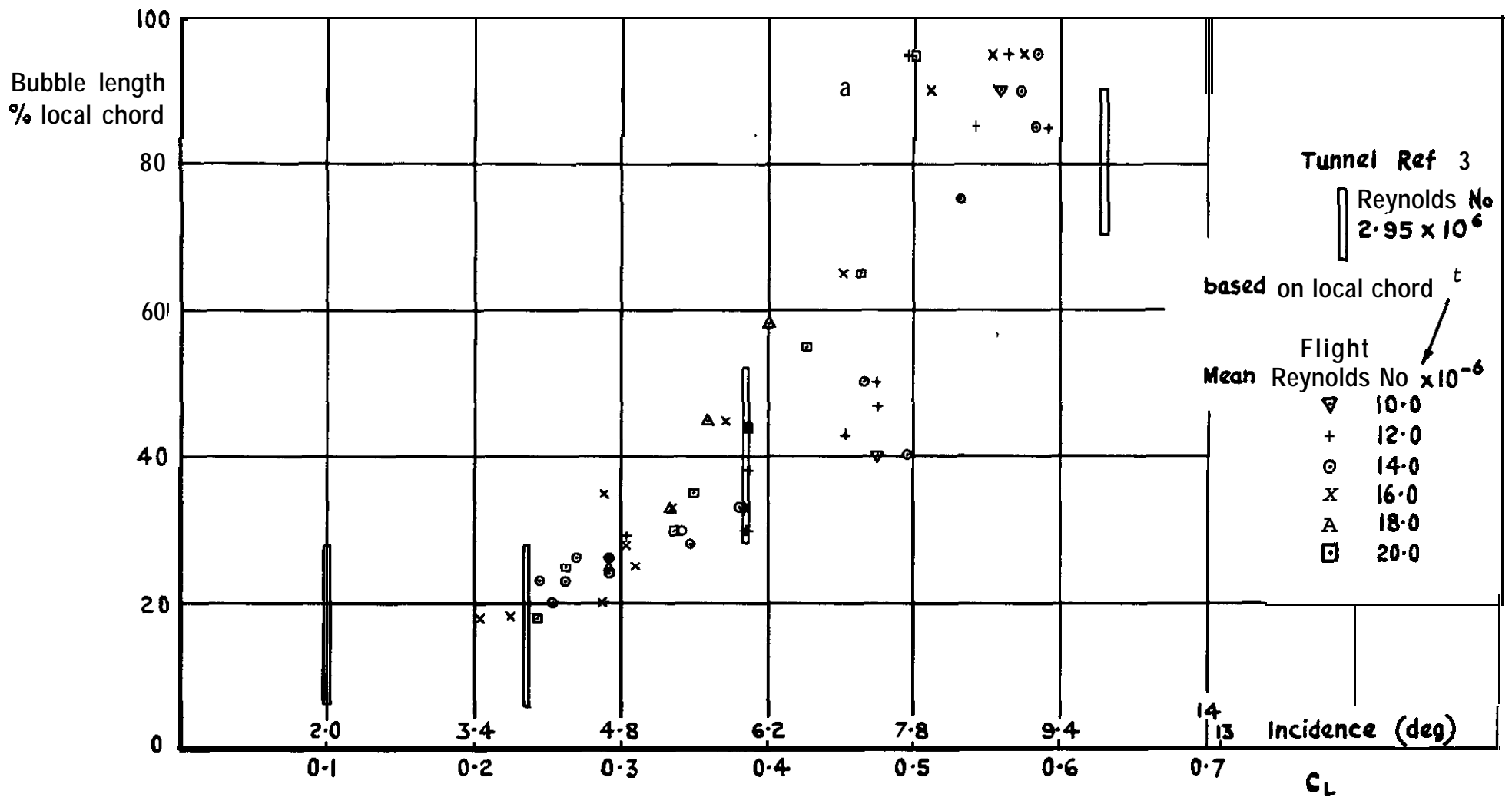


Fig.9 Separation bubble length at the spanwise transducer station versus lift coefficient

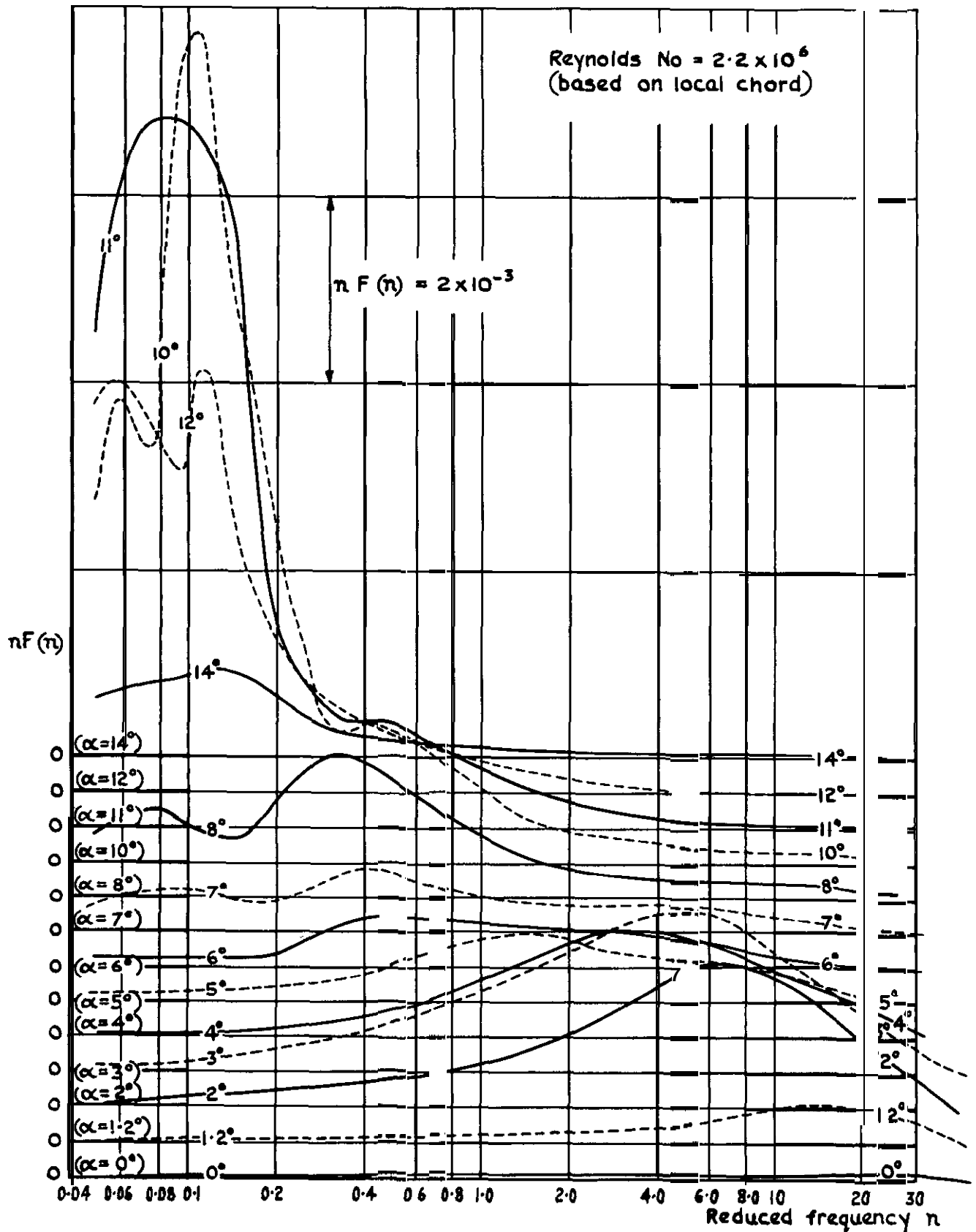


Fig. 10 Power spectra of pressure fluctuations at 10% orifice at various incidences, wind tunnel

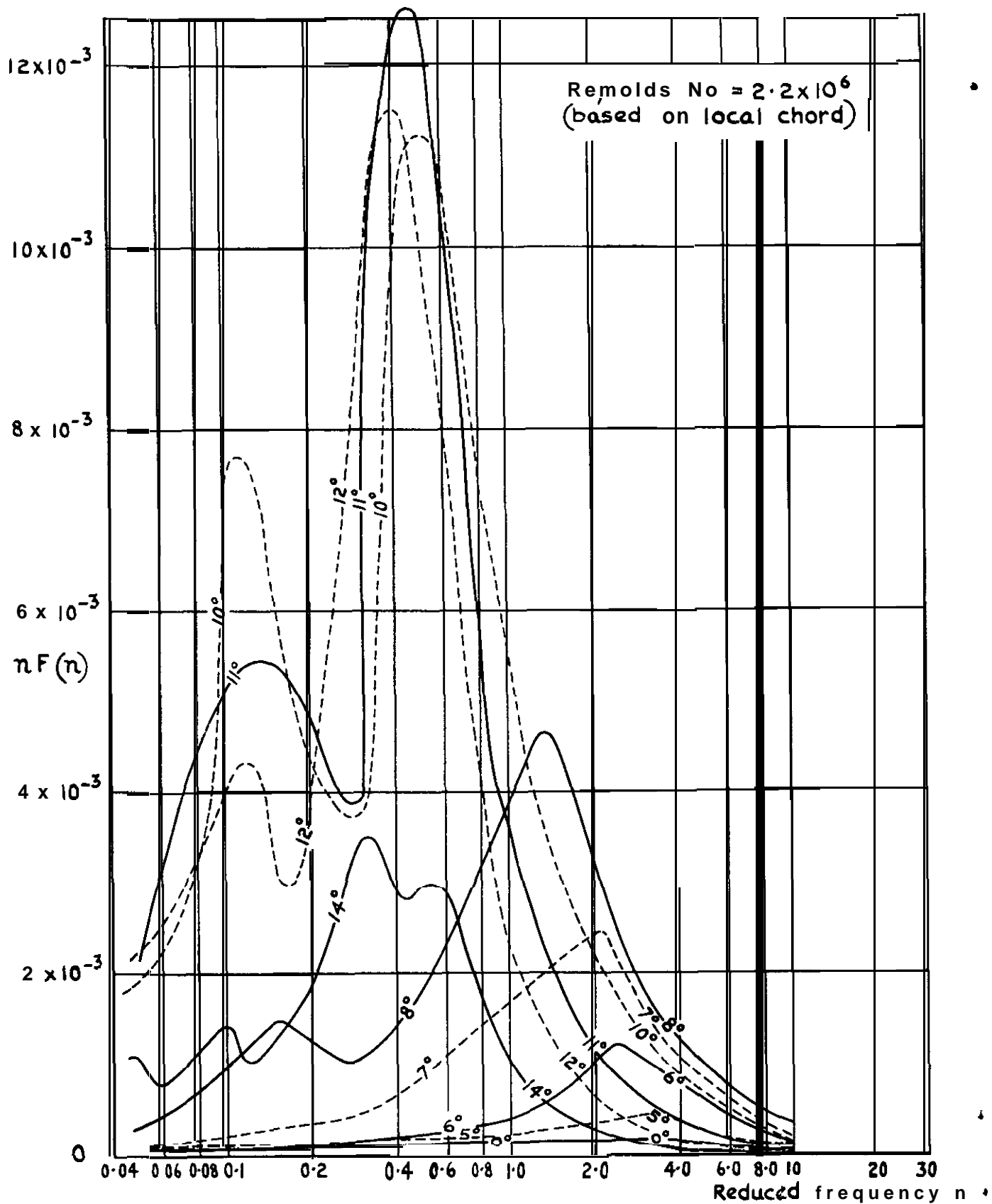


Fig. II Power spectra of pressure fluctuations at 60% orifice at various incidences, wind tunnel

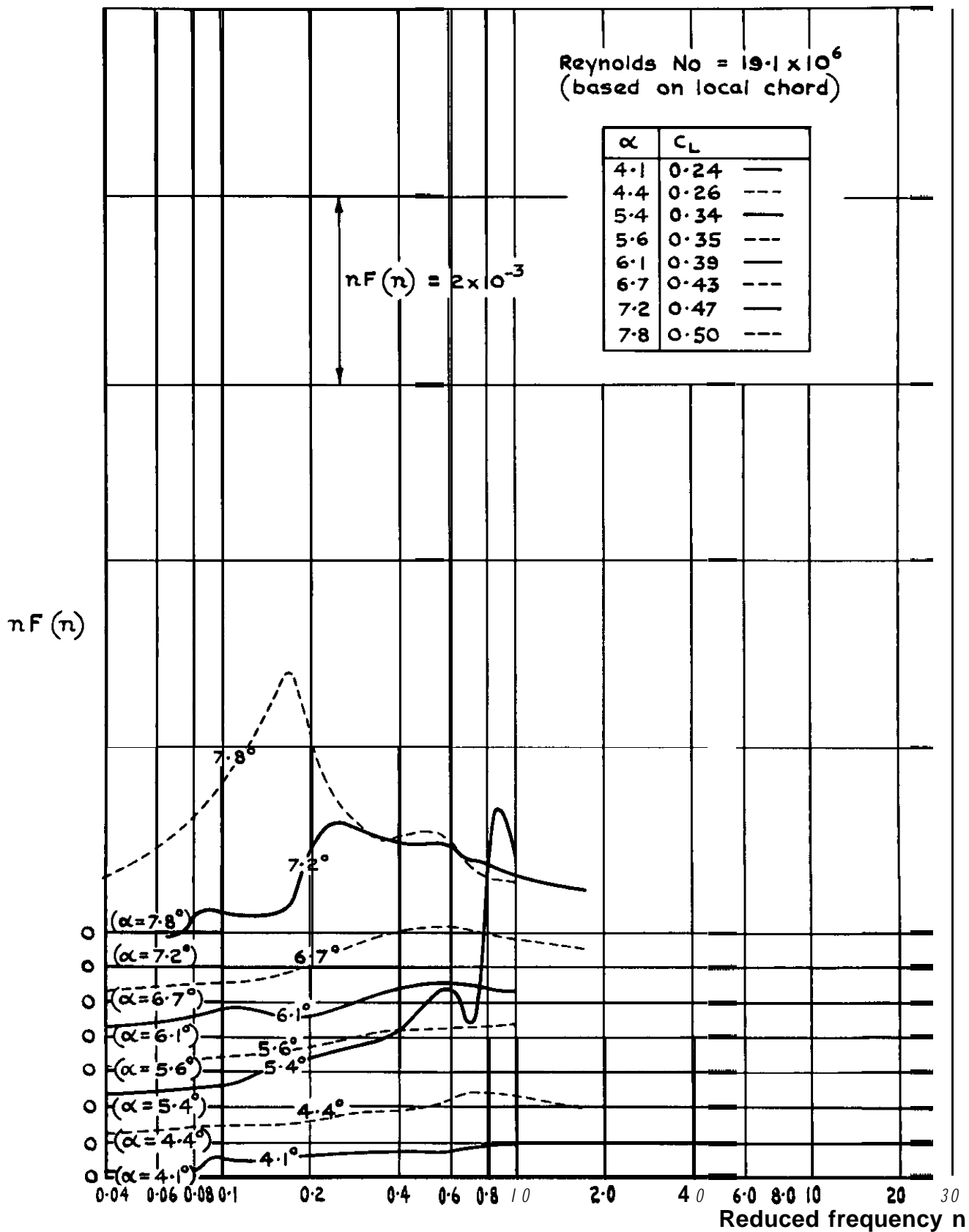


Fig. 12 Power spectra of pressure fluctuations at 10% orifice at various incidences, flight

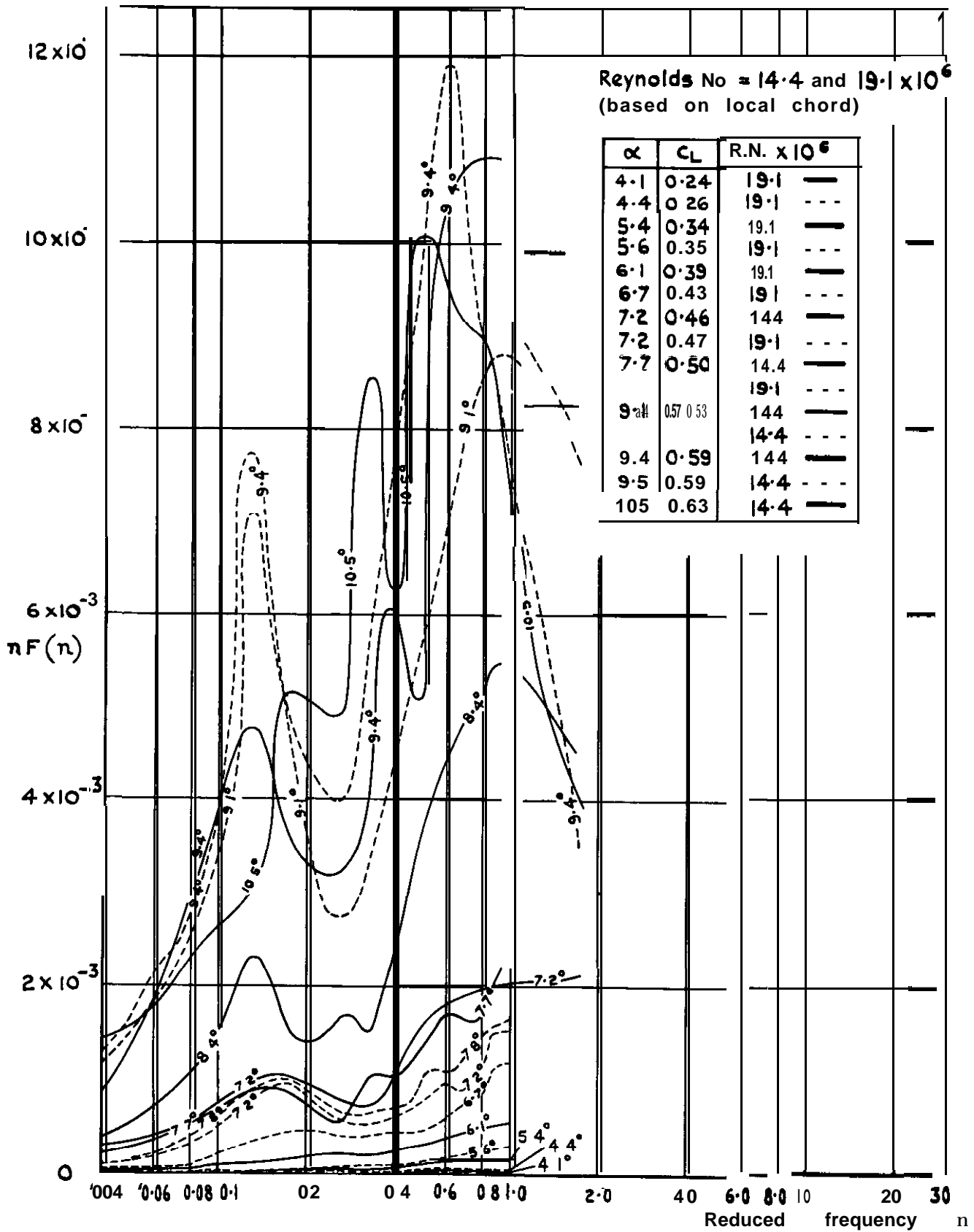


Fig. 13 Power spectra of pressure fluctuations at 60% orifice at various incidences, flight

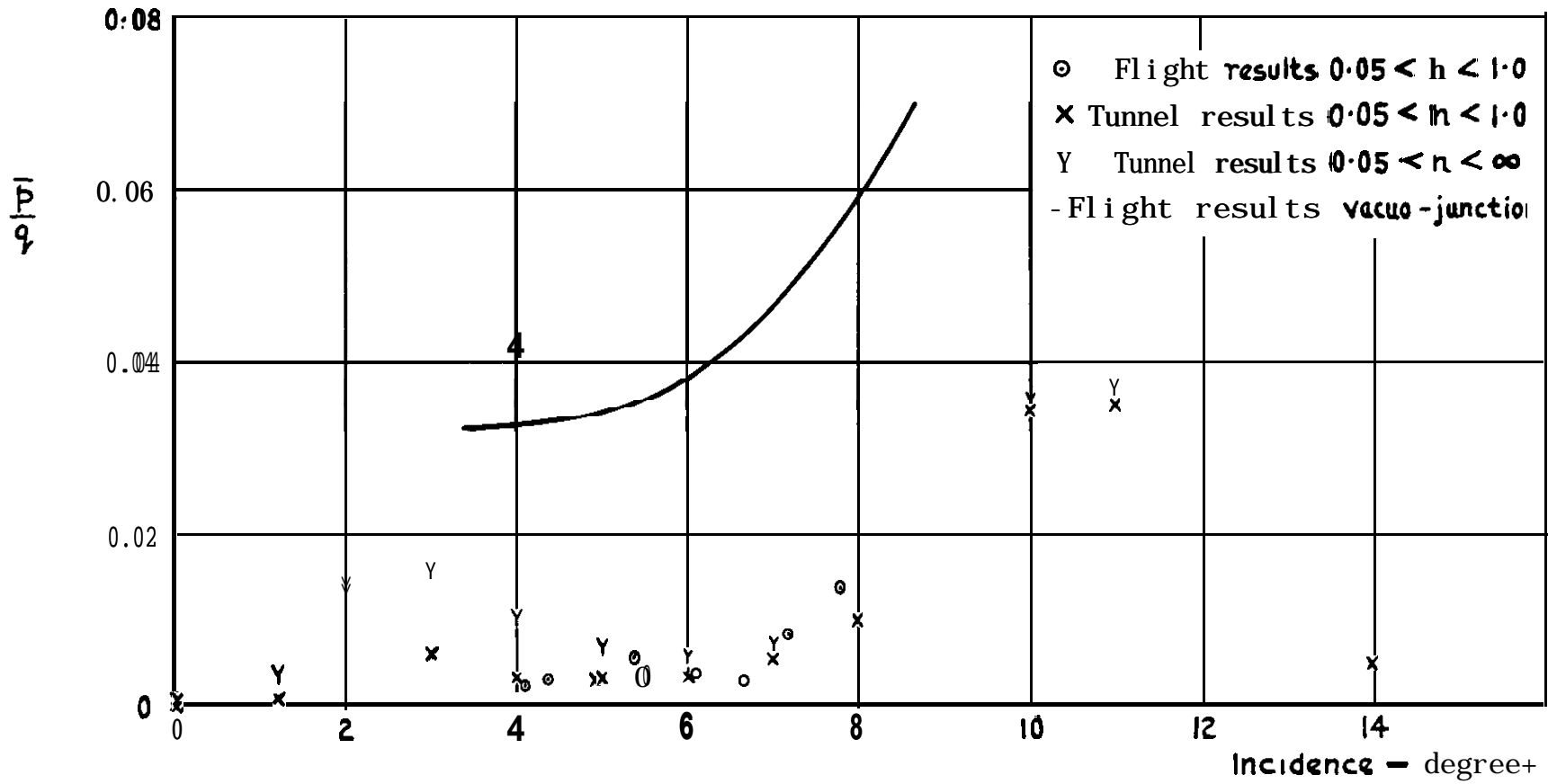


Fig.14 comparison of $\frac{\bar{p}}{q}$ from integroton with vacuo - junction results 10 % orifice

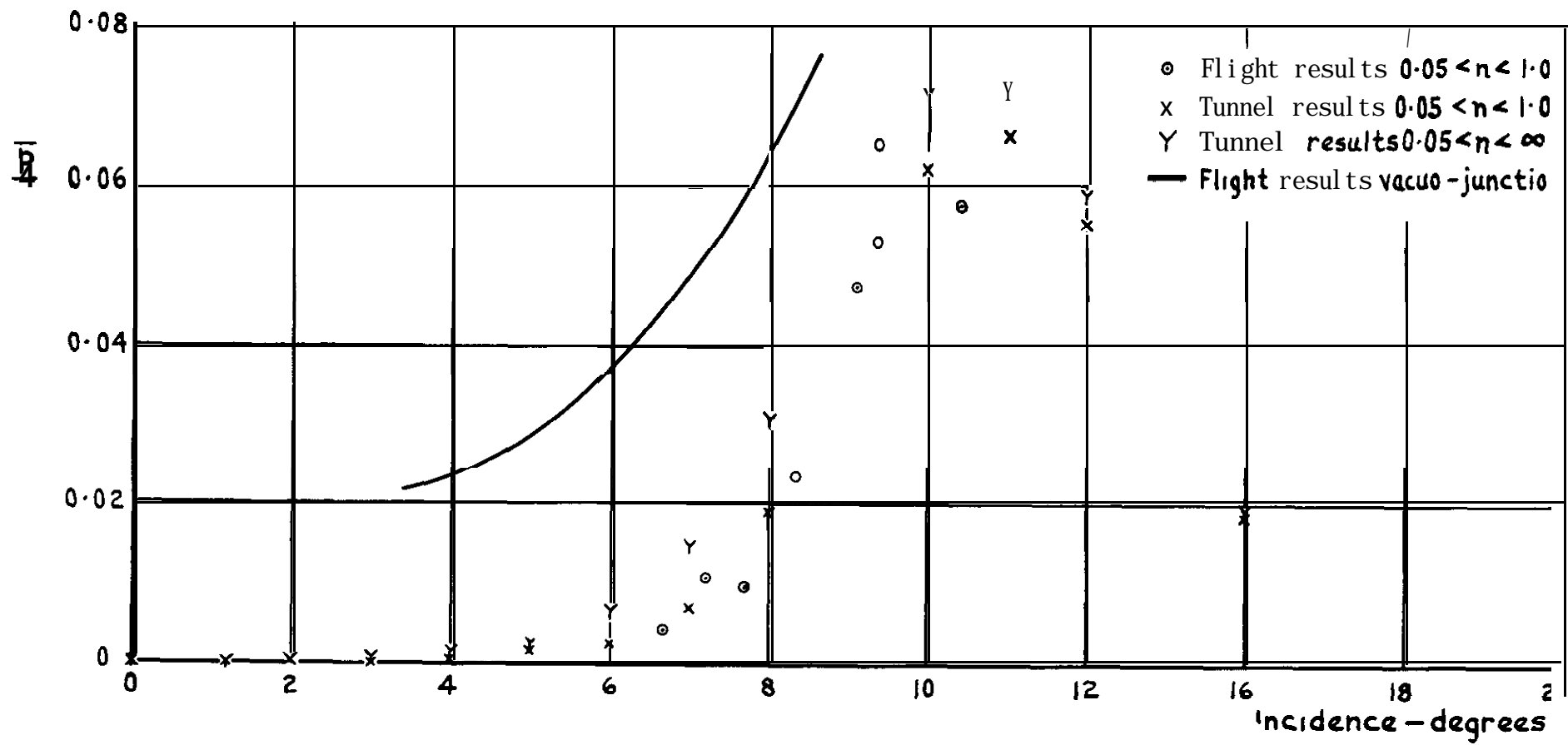


Fig.15 Comparison of $\frac{\bar{P}}{q}$ from integration with vacuo-junctio results 60% orifice

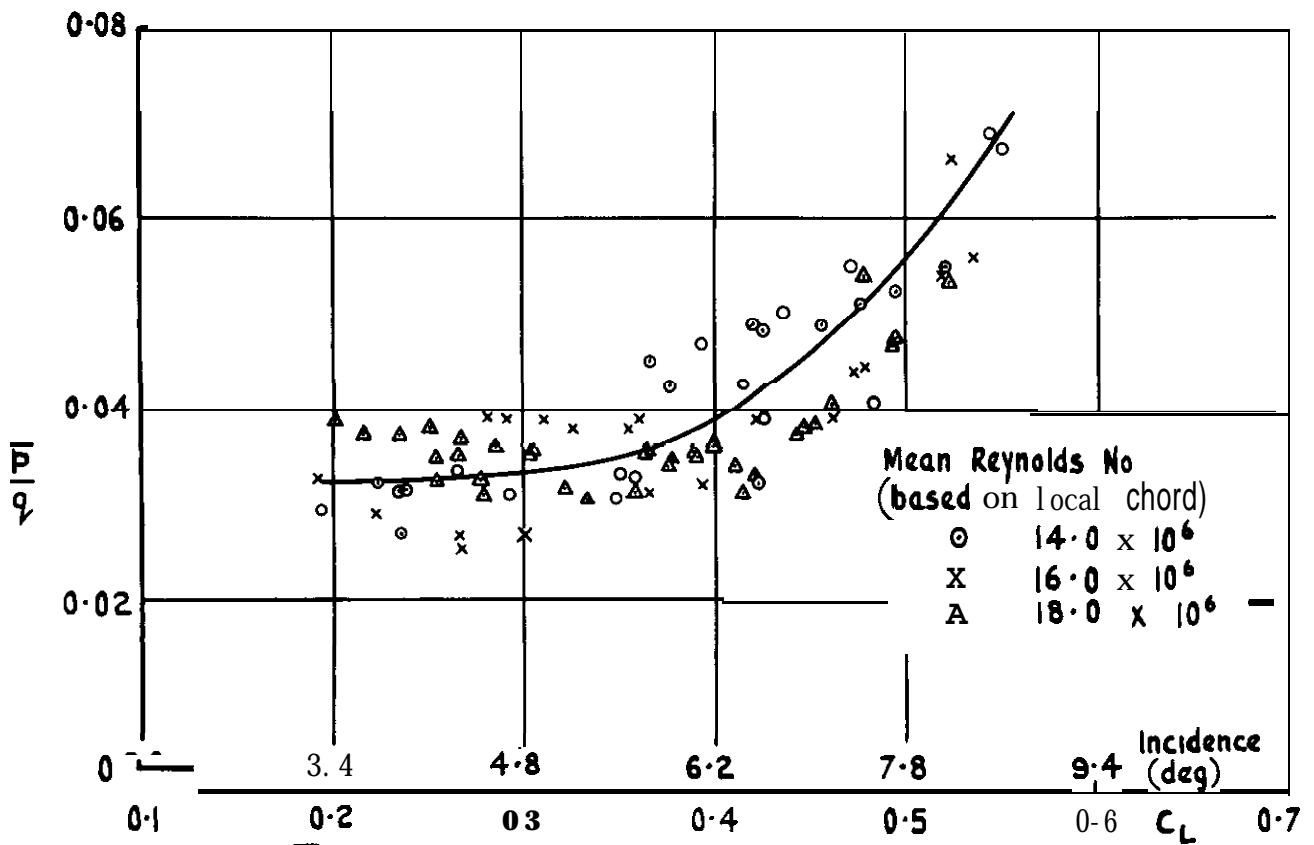


Fig. 16 $\frac{\bar{p}}{q}$ versus C_L for 10% orif ice-vacua -junction

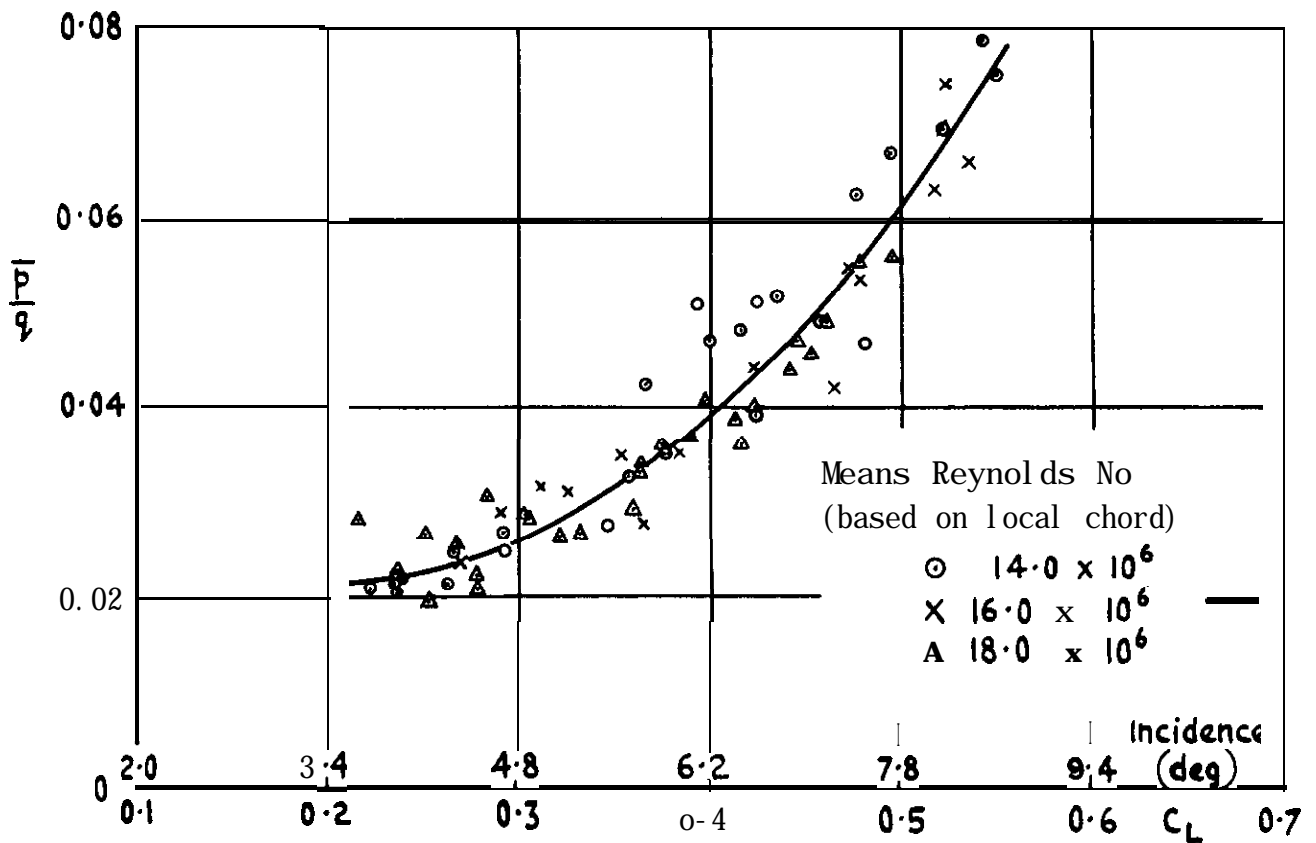


Fig. 17 $\frac{\bar{p}}{q}$ versus C_L for 60% orifice- vacua -junction

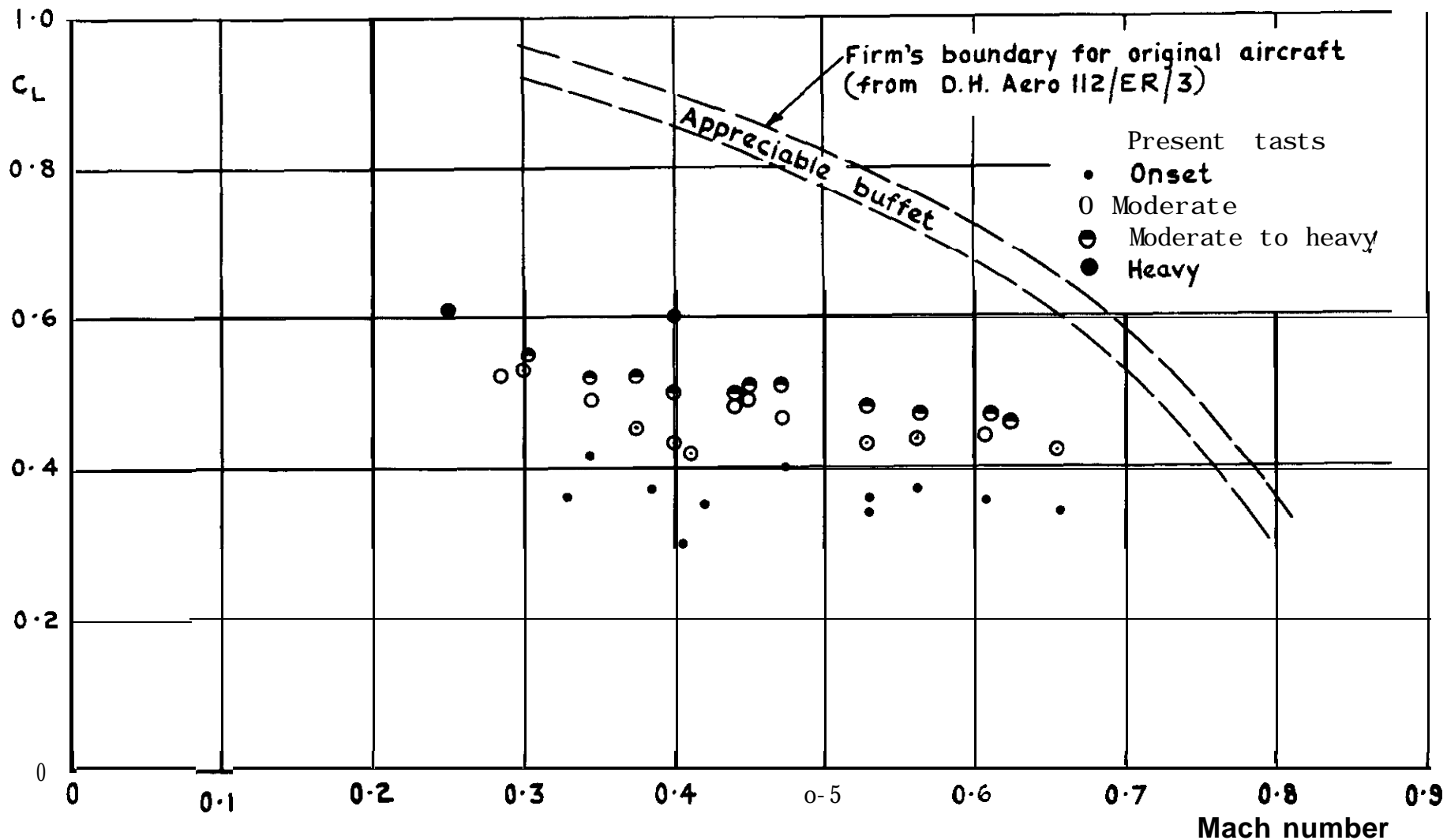


Fig.18 Buffet boundaries of original and modified aircraft

A. R. C. C.P. 1032
November 1967

Rose, R.
Nicholas, O.P.

533.6.071.5 :
533.693 :
533.694.25 :
533.6.054 :
533.6.071

**FLIGHT AND TUNNEL MEASUREMENTS OF PRESSURE FLUCTUATIONS
ON THE UPPER SURFACE OF THE WING OF A VENOM AIRCRAFT
WITH A SHARPENED LEADING-EDGE**

Part span sharpened leading-edges were attached to the wing to produce regions of separated flow. Measurements were made of both the spectra and root-mean-square intensity of the pressure fluctuations at orifices at 10% and 60% of the local chord. Corresponding measurements on a model in a low speed wind tunnel covered a wider range of incidence and frequency than the flight tests. The flight test results are in good agreement with the tunnel results. The root-mean-square value of the pressure fluctuations, \bar{p} , reached a maximum value of $\bar{p}/q = 0.072$ for
(Over)

A.R.C. C.P. 1032
November 1967

Rose, R.
Nicholas, O.P.

533.6.071.5 :
533.693 :
53.694.25 :
533.6.054 :
533.6.071

**FLIGHT AND TUNNEL MEASUREMENTS OF PRESSURE FLUCTUATIONS
ON THE UPPER SURFACE OF THE WING OF A VENOM AIRCRAFT
WITH A SHARPENED LEADING-EDGE**

Part span sharpened leading-edges were attached to the wing to produce regions of separated flow. Flight measurements were made of both the spectra and root-mean-square intensity of the pressure fluctuations at orifices at 10% and 60% of the local chord. Corresponding measurements on a model in a low speed wind tunnel covered a wider range of incidence and frequency than the flight tests. The flight test results are in good agreement with the tunnel results. The root-mean-square value of the pressure fluctuations, \bar{p} , reached a maximum value of $\bar{p}/q = 0.072$ for
(Over)

A. R. C. C.P. 1032
November 1967

Rose, R.
Nicholas, O.P.

533.6.071.5 :
53.693 :
533.694.25 :
533.6.054 :
533.6.071

**FLIGHT AND TUNNEL MEASUREMENTS OF PRESSURE FLUCTUATIONS
ON THE UPPER SURFACE OF THE WING OF A VENOM AIRCRAFT
WITH A SHARPENED LEADING-EDGE**

Part span sharpened leading-edges were attached to the wing to produce regions of separated flow. Flight measurements were made of both the spectra and root-mean-square intensity of the pressure fluctuations at orifices at 10% and 60% of the local chord. Corresponding measurements on a model in a low speed wind tunnel covered a wider range of incidence and frequency than the flight tests. The flight test results are in good agreement with the tunnel results. The root-mean-square value of the pressure fluctuations, \bar{p} , reached a maximum value of $\bar{p}/q = 0.072$ for
(Over)

the 60% orifice at an incidence of 10° . The incidence for buffet onset was close to that at which the break in the \bar{p}/q vs. α curves for both orifices occurred.

the 60% orifice at an incidence of 10° . The incidence for buffet onset was close to that at which the break in the \bar{p}/q vs. α curves for both orifices occurred.

the 60% orifice at an incidence of 10° . The incidence for buffet onset was close to that at which the break in the \bar{p}/q vs. α curves for both orifices occurred.

11

12

13

© Crown *copyright* 1969

Published by

HER MAJESTY'S STATIONERY OFFICE

To be purchased from

49 High Holborn, London WC1

13A Castle Street, Edinburgh 2

109 St Mary Street, Cardiff CF1 1JW

Brazenose street, Manchester 2

50 Fairfax Street, Bristol BS1 3DE

258 Broad Street, Birmingham 1

7 Linenhall Street, Belfast BT2 8AY

or through any bookseller